

Strength of dx²-y² pairing in the two-leg Hubbard ladder

著者	前川 禎通
journal or publication title	Physical review. B
volume	74
number	13
page range	132503-1-132503-1
year	2006
URL	http://hdl.handle.net/10097/40340

doi: 10.1103/PhysRevB.74.132503

Strength of $d_{x^2-y^2}$ pairing in the two-leg Hubbard ladder

N. Bulut and S. Maekawa

Institute for Materials Research, Tohoku University, Sendai 980-8577, Japan

and CREST, Japan Science and Technology Agency (JST), Kawaguchi, Saitama 332-0012, Japan

(Received 20 September 2005; revised manuscript received 25 August 2006; published 11 October 2006)

In the ground state of the doped two-leg Hubbard ladder there are power-law decaying $d_{x^2-y^2}$ -type pairing correlations. It is important to know the strength and the temperature scale of these correlations. For this purpose, we have performed determinantal quantum Monte Carlo (QMC) calculations of the reducible particle-particle interaction in the Hubbard ladder. In this paper, we report on these calculations and show that, at sufficiently low temperatures, resonant particle-particle scattering takes place in the $d_{x^2-y^2}$ pairing channel for certain values of the model parameters. The QMC data presented here indicate that the $d_{x^2-y^2}$ pairing correlations are strong in the Hubbard ladder.

DOI: [10.1103/PhysRevB.74.132503](https://doi.org/10.1103/PhysRevB.74.132503)

PACS number(s): 71.10.Fd, 71.10.Li, 74.20.Rp

It is generally accepted that the high- T_c cuprates¹ are $d_{x^2-y^2}$ wave superconductors.^{2,3} It is also known that the spin-fluctuation exchange in electronic models^{4,5} and an electron-phonon interaction which has its largest coupling at small wave vectors⁶⁻⁸ can lead to an effective electron-electron interaction which is attractive in the d -wave Bardeen-Cooper-Schrieffer (BCS) pairing channel. However, it is not yet clear what is the pairing interaction responsible for superconductivity in the high- T_c cuprates. Within this context, it is important to determine the maximum possible strength of the $d_{x^2-y^2}$ pairing correlations which one can obtain in a purely electronic model such as the Hubbard model. Unfortunately, the ground state of the two-dimensional (2D) Hubbard model remains beyond the reach of the exact many-body techniques.⁹ However, in the case of the two-leg Hubbard ladder, the density matrix renormalization group (DMRG) calculations found power-law decaying $d_{x^2-y^2}$ -type pair-field correlations.^{10,11} This is probably the only model where it is known from exact calculations that the pairing correlations become enhanced by turning on an onsite Coulomb repulsion in the ground state.^{11,12} Hence, it is important to determine the maximum possible strength and the temperature scale of the $d_{x^2-y^2}$ pairing correlations in the Hubbard ladder, which is the main motivation of this paper.

Here, we present quantum Monte Carlo (QMC) results on the reducible particle-particle interaction Γ in the BCS channel, which is illustrated in Fig. 1. The reducible Γ serves as a powerful probe of the pairing correlations. For example, in the case of an s -wave superconductor, Γ at the Fermi surface would diverge to $-\infty$ due to repeated particle-particle scatterings in the BCS channel, when the superconducting transition is approached, $T \rightarrow T_c^+$. In this paper, we investigate the strength of the $d_{x^2-y^2}$ pairing in the Hubbard ladder by making use of the exact QMC data on Γ .

In the following, we show that the reducible particle-particle interaction Γ in the Hubbard ladder exhibits diverging behavior as the temperature is lowered for certain values of the model parameters. We find that, on the Fermi surface, Γ can become strongly repulsive (attractive) for $\mathbf{q} \approx (\pi, \pi)$ ($\mathbf{q} \approx 0$) momentum transfers, which correspond to backward (forward) scatterings. In particular, near half-filling and for Coulomb repulsion $U=4t$ and temperature $T=0.1t$, where t is

the hopping matrix element, the backward and forward scattering amplitudes can become an order of magnitude larger than the bare Coulomb repulsion or the bare bandwidth. This type of momentum dependence of Γ implies that resonant particle-particle scattering is taking place in the BCS channel already at $T \approx 0.1t$. For $U=8t$, we observe similar behavior at about twice higher temperatures. The temperatures studied in this paper are lower than those reached in previous QMC calculations of Γ for the 2D (Ref. 13) and the two-leg¹⁴ Hubbard models. In addition, we present results on the solution of the Bethe-Salpeter equation in the BCS channel, which quantitatively determines the strength of the pairing correlations. The QMC data shown in this paper imply that the $d_{x^2-y^2}$ -type pairing in the two-leg Hubbard ladder is strong for certain values of the model parameters.

We begin by briefly describing the previous studies of $d_{x^2-y^2}$ pairing in the Hubbard ladder. The DMRG calculations found that the rung-rung pair-field correlation function decays as power law in the ground state of the doped Hubbard ladder.¹⁰ The mean-field calculations suggested the $d_{x^2-y^2}$ type of symmetry for pairing in doped spin ladders.¹⁵ The exact diagonalization¹² and the DMRG¹¹ calculations found that the $d_{x^2-y^2}$ pairing correlations are most enhanced when the interchain hopping t_\perp is greater than the intrachain hopping t , in particular, for $t_\perp \approx 1.5t$ in the intermediate coupling regime and near half-filling. In this case, the QMC calculations showed that the irreducible particle-particle interaction peaks for momentum transfers near (π, π) due to antiferromagnetic fluctuations.¹⁴

The two-leg Hubbard model is defined by

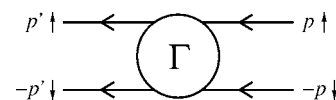


FIG. 1. Feynman diagram for the reducible particle-particle interaction $\Gamma(p'|p)$ in the BCS channel. Here, p denotes $(\mathbf{p}, i\omega_n)$ with Matsubara frequency ω_n . In this diagram, the incoming fermions at states p with up spin and $-p$ with down spin scatter to states p' with up spin and $-p'$ with down spin by exchanging $q=p'-p$.

$$\begin{aligned}
H = & -t \sum_{i,\lambda,\sigma} (c_{i,\lambda,\sigma}^\dagger c_{i+1,\lambda,\sigma} + \text{H.c.}) \\
& -t_\perp \sum_{i,\sigma} (c_{i,1,\sigma}^\dagger c_{i,2,\sigma} + \text{H.c.}) + U \sum_{i,\lambda} n_{i,\lambda,\uparrow} n_{i,\lambda,\downarrow} \\
& -\mu \sum_{i,\lambda,\sigma} n_{i,\lambda,\sigma},
\end{aligned} \tag{1}$$

where t is the hopping parameter parallel to the chains (along \hat{x}), and t_\perp is for hopping perpendicular to the chains (along \hat{y}). The operator $c_{i,\lambda,\sigma}^\dagger$ ($c_{i,\lambda,\sigma}$) creates (annihilates) an electron of spin σ at site i of chain λ , and $n_{i,\lambda,\sigma} = c_{i,\lambda,\sigma}^\dagger c_{i,\lambda,\sigma}$ is the electron occupation number. As usual, U is the onsite Coulomb repulsion, and μ is the chemical potential. In addition, periodic boundary conditions were used along the chains, and t_\perp denotes interchain hopping for open boundary conditions.

In obtaining the data presented here, the determinantal QMC technique described in Ref. 16 was used. The calculation of the reducible interaction Γ follows the procedure described in Ref. 13 for the 2D case. The BCS component of the reducible particle-particle interaction $\Gamma(p'|p)$ is illustrated in Fig. 1, where $p = (\mathbf{p}, i\omega_n)$ with Matsubara frequency $\omega_n = (2n+1)\pi T$. In the following, results will be shown for the reducible interaction in the singlet channel, $\Gamma_s(p'|p) = \frac{1}{2}[\Gamma(p'|p) + \Gamma(-p'|p)]$. In particular, the momentum dependence of $\Gamma_s(\mathbf{p}', i\omega_{n'} | \mathbf{p}, i\omega_n)$ will be shown at the lowest Matsubara frequency $\omega_n = \omega_{n'} = \pi T$. In the ground state and for $U=4t$, the $d_{x^2-y^2}$ -type pairing correlations are most enhanced near half-filling for $t_\perp \approx 1.6t$.¹¹ When $U=8t$, this occurs for $t_\perp \approx 1.4t$. In this paper, the QMC data will be presented using these two parameter sets for a 2×16 lattice.

The momentum structure in $\Gamma_s(p'|p)$ depends sensitively on where \mathbf{p}' and \mathbf{p} are located with respect to the Fermi surface. Hence, we will first show results on the single-particle spectral weight $A(\mathbf{p}, \omega) = -\frac{1}{\pi} \text{Im} G(\mathbf{p}, \omega + i\delta)$, where G is the single-particle Green's function. Our purpose here is to find the locations of the Fermi-surface crossing points. We have obtained $A(\mathbf{p}, \omega)$ from the QMC data on the single-particle Green's function along the Matsubara-time axis by using the maximum-entropy analytic continuation method. Figure 2 shows $A(\mathbf{p}, \omega)$ vs ω for $T=0.1t$, $U=4t$, $t_\perp=1.6t$, and $\langle n \rangle = 0.94$. Here, we see that the Fermi level crossing for the antibonding ($p_y = \pi$) band occurs for p_x between $\pi/8$ and $\pi/4$, while for the bonding ($p_y = 0$) band there is spectral weight pinned near the Fermi level for $3\pi/4 \leq p_x \leq \pi$ at this temperature. These results for $A(\mathbf{p}, \omega)$ are similar to those presented in Refs. 11 and 14. In the following, $\Gamma_s(\mathbf{p}', i\pi T | \mathbf{p}, i\pi T)$ vs \mathbf{p} will be shown for $\mathbf{p}' = (\pi/4, \pi)$ near the Fermi level and for $\mathbf{p}' = (0, \pi)$ at the saddle point.

Figure 3(a) shows $\Gamma_s(\mathbf{p}', i\pi T | \mathbf{p}, i\pi T)$ vs \mathbf{p} while \mathbf{p}' is kept fixed at $(\pi/4, \pi)$. In the left panel, p_x is scanned from $-\pi$ to π for $p_y=0$, while in the right panel p_x is scanned for $p_y=\pi$. Here, it is seen that repulsive and attractive peaks develop in Γ_s , as T decreases from $0.25t$ to $0.1t$. In particular, in the left panel it is seen that when $\mathbf{p} \approx (-3\pi/4, 0)$ a repulsive peak develops in Γ_s , which corresponds to a scattering process with momentum transfer $\mathbf{q} \approx (\pi, \pi)$. In addition, in

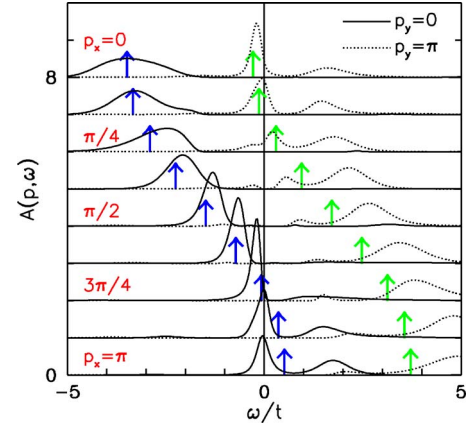


FIG. 2. (Color online) Single-particle spectral weight $A(\mathbf{p}, \omega)$ vs ω at various \mathbf{p} . The solid and dotted curves represent the bonding ($p_y=0$) and antibonding ($p_y=\pi$) bands, respectively. These results are for $T=0.1t$, $U=4t$, $t_\perp=1.6t$, and $\langle n \rangle = 0.94$. The arrows denote the quasiparticle positions for the $U=0$ case.

the right panel it is observed that a dip develops in Γ_s when $\mathbf{p} \approx \mathbf{p}' = (\pi/4, \pi)$ corresponding to zero momentum transfer. This dip is due to resonant scattering in the $d_{x^2-y^2}$ wave BCS channel. In a three-dimensional infinite system, when a $d_{x^2-y^2}$ wave superconducting instability is approached, $\Gamma_s(\mathbf{p}', i\pi T | \mathbf{p}, i\pi T)$ at the Fermi level diverges to $+\infty$ for backward scattering, and to $-\infty$ for forward scattering, which will be further discussed below. In Fig. 3(a) it is seen that Γ_s is developing this type of repulsive and attractive peaks at T of order $0.1t$.

Figure 3(b) shows $\Gamma_s(\mathbf{p}', i\pi T | \mathbf{p}, i\pi T)$ vs \mathbf{p} while \mathbf{p}' is kept fixed at the saddle point $(0, \pi)$. In this case, Γ_s develops a peak when $\mathbf{p} = (\pm\pi, 0)$, corresponding to scattering with

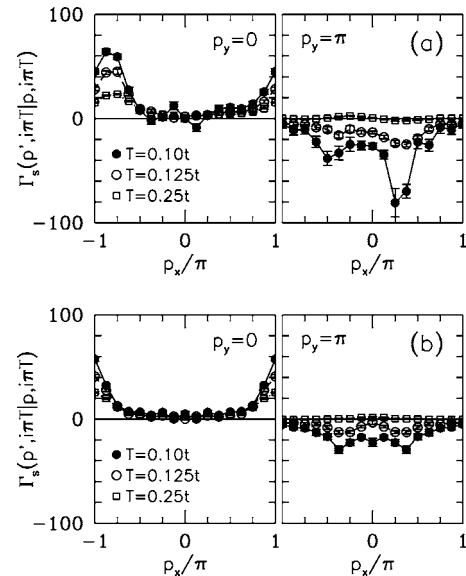


FIG. 3. Reducible particle-particle interaction in the singlet channel $\Gamma_s(\mathbf{p}', i\pi T | \mathbf{p}, i\pi T)$ vs p_x . Here, p_x is scanned for $p_y=0$ (left panel) and for $p_y=\pi$ (right panel). In (a), \mathbf{p}' is kept fixed at $(\pi/4, \pi)$, while in (b), $\mathbf{p}' = (0, \pi)$. Here, Γ_s is shown in units of t for $U=4t$, $t_\perp=1.6t$, and $\langle n \rangle = 0.94$.

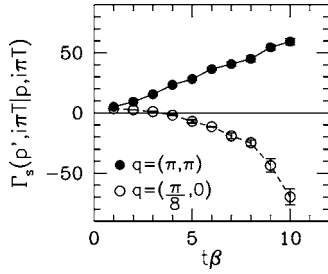


FIG. 4. Reducible particle-particle interaction in the singlet channel $\Gamma_s(\mathbf{p}', i\pi T | \mathbf{p}, i\pi T)$ vs the inverse temperature β for backward [$\mathbf{q}=(\pi, \pi)$] and forward [$\mathbf{q}=(\pi/8, 0)$] scatterings. Here, $\mathbf{p}=\mathbf{p}'+\mathbf{q}$ and \mathbf{p}' is kept fixed at $(\pi/4, \pi)$. These results are for $U=4t$, $t_\perp=1.6t$, and $\langle n \rangle=0.94$.

$\mathbf{q}=(\pi, \pi)$ momentum transfer. The magnitude of this peak is comparable to that seen in the left panel of Fig. 3(a). However, the behavior for $\mathbf{q}=0$ momentum transfer is different. As observed in the right panel of Fig. 3(b), Γ_s for $\mathbf{q}=0$ scattering remains pinned near zero for T down to $0.125t$, and becomes attractive only below this temperature. Hence, at the saddle point $(0, \pi)$, the resonant scattering in Γ_s for $\mathbf{q}=0$ momentum transfer is weaker compared to that at $(\pi/4, \pi)$.

Figure 4 shows the T dependence of the backward and forward scattering components of Γ_s . Here, Γ_s is plotted as a function of the inverse temperature β for momentum transfers $\mathbf{q}=(\pi, \pi)$ and $(\pi/8, 0)$, while \mathbf{p}' is kept fixed at $(\pi/4, \pi)$. This figure shows that, near the Fermi level, the backward and forward scattering amplitudes increase rapidly at low T , becoming an order of magnitude larger than the bare Coulomb repulsion at $T \approx 0.1t$.

Figures 3 and 4 display the main features of Γ_s , which can be summarized as follows: At low T , there are strong $\mathbf{q} \approx (\pi, \pi)$ scatterings over the whole Brillouin zone, while the $\mathbf{q} \approx 0$ scatterings are most attractive near the Fermi surface. These features were observed at $\langle n \rangle=0.94$ and 0.875 , and for $U=4t$ and $8t$. The one-loop renormalization-group (RG) technique is also utilized to obtain the momentum dependence of Γ in the Hubbard model.^{17,18} It would be useful to make comparisons of the QMC and the RG results for the momentum dependence of Γ in the ladder case and to relate the peaks in Γ with the relevant couplings in the RG calculations.

In order to determine the strength of the pairing correlations, the Bethe-Salpeter equation for the reducible particle-particle interaction in the BCS channel,

$$\frac{\lambda_\alpha}{1-\lambda_\alpha} \phi_\alpha(p) = -\frac{T}{N} \sum_{p'} \Gamma(p|p') |G(p')|^2 \phi_\alpha(p'), \quad (2)$$

was solved for λ_α and the corresponding eigenfunctions $\phi_\alpha(\mathbf{p}, i\omega_n)$ by using QMC data on Γ and the single-particle Green's function $G(p)$. For a three-dimensional infinite system, when the maximum λ_α reaches 1, this signals a BCS instability to a state where the pair wave function has the form of the corresponding eigenfunction. For a one-dimensional system, λ_α 's will always be less than 1, how-

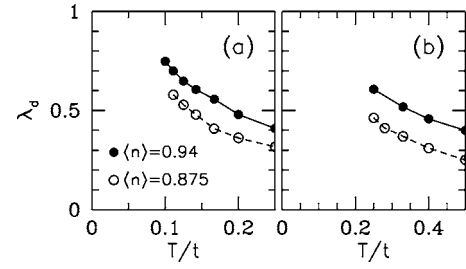


FIG. 5. d -wave irreducible eigenvalue λ_d of the Bethe-Salpeter equation vs T (a) for $U=4t$ and $t_\perp=1.6t$, and (b) for $U=8t$ and $t_\perp=1.4t$. Here, the errorbars are smaller than the size of the symbols.

ever, the T dependence of λ_α 's gives information about the characteristic temperature scale of the pairing correlations. For instance, if the maximum eigenvalue reaches 0.9 at some temperature, then this means that the leading pairing correlations are enhanced by a factor of 10 through repeated particle-particle scatterings in the BCS channel. Hence, at this temperature, the system would exhibit strong pairing fluctuations.¹⁹

At low temperatures, the maximum λ_α of the Bethe-Salpeter equation corresponds to an eigenfunction $\phi_d(\mathbf{p}, i\omega_n)$ which has $d_{x^2-y^2}$ type of symmetry in the sense that it changes sign as \mathbf{p} goes from $(\pi, 0)$ to $(0, \pi)$ in the Brillouin zone.¹⁴ The temperature evolution of the $d_{x^2-y^2}$ wave irreducible eigenvalue λ_d is shown in Fig. 5(a) for $U=4t$ and $t_\perp=1.6t$. As T decreases, λ_d grows monotonically reaching 0.75 at $T=0.1t$ for $\langle n \rangle=0.94$. The simple extrapolation of these results suggests that λ_d will reach 0.9 at $T > 0.05t$ for $\langle n \rangle=0.94$. At the temperatures where these calculations were performed, λ_d decreases upon doping to $\langle n \rangle=0.875$. Because of the QMC “fermion sign problem,”²⁰ these data were obtained by using parallel computers. Also shown in Fig. 5(b) is λ_d for $U=8t$ and $t_\perp=1.4t$. We find that, at $T \geq 0.25t$, λ_d takes larger values for $U=8t$ than for $U=4t$. These results indicate that the $d_{x^2-y^2}$ pairing correlations are strong in the Hubbard ladder.

An important feature of the QMC data presented here is that, at sufficiently low T , Γ_s near the Fermi level becomes strongly attractive for $\mathbf{q} \approx 0$ momentum transfers. This is due to resonant scattering in the $d_{x^2-y^2}$ wave BCS channel. In order to demonstrate this effect, consider the case of an irreducible interaction Γ_1 which is independent of frequency and separable in momentum,

$$\Gamma_1(\mathbf{p}' | \mathbf{p}) = \sum_{\alpha} V_{\alpha} g_{\alpha}(\mathbf{p}') g_{\alpha}(\mathbf{p}), \quad (3)$$

where α denotes the various pairing channels. In this case, the reducible interaction is given by

$$\Gamma(\mathbf{p}' | \mathbf{p}) = \sum_{\alpha} \frac{V_{\alpha}}{1 - V_{\alpha} P_{\alpha}} g_{\alpha}(\mathbf{p}') g_{\alpha}(\mathbf{p}), \quad (4)$$

with $P_{\alpha} = -(T/N) \sum_{p} g_{\alpha}^2(\mathbf{p}) |G(p)|^2$. In general, Γ_1 has both attractive and repulsive V_{α} . In Eq. (4), it is seen that the repulsive components become suppressed by repeated scatterings in the BCS channel, while the attractive components become

enhanced. For the $d_{x^2-y^2}$ channel, $g_d(\mathbf{p}) = \frac{1}{2}(\cos p_x - \cos p_y)$. If the $d_{x^2-y^2}$ component of Γ_1 is attractive and becomes sufficiently enhanced, here it is observed that Γ for $\mathbf{q} = \mathbf{p}' - \mathbf{p} \approx 0$ can become attractive. When a $d_{x^2-y^2}$ wave BCS instability is approached, then, at the Fermi surface, Γ_s diverges to $-\infty$ for $\mathbf{q} \approx 0$ scatterings and to $+\infty$ for $\mathbf{q} \approx (\pi, \pi)$ scatterings. The important point is that the exact QMC data for Γ_s also exhibit this type of momentum dependence in the Hubbard ladder at temperatures which are not low.

In summary, we have presented QMC data on the reducible particle-particle interaction Γ_s in order to determine the strength and the temperature scale of the $d_{x^2-y^2}$ pairing correlations in the two-leg Hubbard ladder. We found that Γ_s displays diverging behavior as the temperature decreases. In particular, Γ_s exhibits resonant scattering in the $d_{x^2-y^2}$ pairing channel as it would be expected for a system near a $d_{x^2-y^2}$ BCS instability. We have also shown results on the solution of the Bethe-Salpeter equation to quantitatively determine the strength of the $d_{x^2-y^2}$ pairing. The QMC data presented in this paper indicate that the $d_{x^2-y^2}$ pairing correlations in the

Hubbard ladder are strong for certain values of the model parameters. We note that, for comparison, it would be useful to investigate the strength of $d_{x^2-y^2}$ pairing for a two-leg ladder system which includes both onsite Coulomb and electron-phonon interactions.

The authors thank C. Honerkamp, Z. X. Shen, and T. Tohyama for helpful discussions. Part of the numerical calculations reported in this paper were carried out at the ULAKBIM High Performance Computing Center at the Turkish Scientific and Technical Research Council. One of us (N.B.) would like to thank the International Frontier Center for Advanced Materials at Tohoku University for its kind hospitality, and gratefully acknowledges support from the Japan Society for the Promotion of Science and the Turkish Academy of Sciences (Grant No. EA-TUBA-GEBIP/2001-1-1). This work was supported by Priority-Areas Grants from the Ministry of Education, Science, Culture and Sport of Japan, NAREGI Japan, and NEDO.

¹J. G. Bednorz and K. A. Müller, *Z. Phys. B: Condens. Matter* **64**, 189 (1986).

²D. J. Scalapino, *Phys. Rep.* **250**, 330 (1994).

³C. C. Tsuei and J. R. Kirtley, *Rev. Mod. Phys.* **72**, 969 (2000).

⁴K. Miyake, S. Schmitt-Rink, and C. M. Varma, *Phys. Rev. B* **34**, 6554 (1986).

⁵D. J. Scalapino, E. Loh, and J. E. Hirsch, *Phys. Rev. B* **34**, 8190 (1986).

⁶R. Zeyher and M. L. Kulić, *Phys. Rev. B* **53**, 2850 (1996).

⁷N. Bulut and D. J. Scalapino, *Phys. Rev. B* **54**, 14971 (1996).

⁸Z. B. Huang, W. Hanke, E. Arrighoni, and D. J. Scalapino, *Phys. Rev. B* **68**, 220507(R) (2003).

⁹N. Bulut, *Adv. Phys.* **51**, 1587 (2002).

¹⁰R. M. Noack, S. R. White, and D. J. Scalapino, *Phys. Rev. Lett.* **73**, 882 (1994).

¹¹R. M. Noack, N. Bulut, D. J. Scalapino, and M. G. Zacher, *Phys.*

Rev. B **56**, 7162 (1997).

¹²K. Yamaji and Y. Shimoi, *Physica C* **222**, 349 (1994).

¹³N. Bulut, D. J. Scalapino, and S. R. White, *Phys. Rev. B* **47**, R6157 (1993); *Physica C* **246**, 85 (1995).

¹⁴T. Dahm and D. J. Scalapino, *Physica C* **288**, 33 (1997).

¹⁵S. Gopalan, T. M. Rice, and M. Sigrist, *Phys. Rev. B* **49**, 8901 (1994).

¹⁶S. R. White *et al.*, *Phys. Rev. B* **40**, 506 (1989).

¹⁷N. Furukawa, T. M. Rice, and M. Salmhofer, *Phys. Rev. Lett.* **81**, 3195 (1998).

¹⁸C. Honerkamp, M. Salmhofer, N. Furukawa, and M. Rice, *Phys. Rev. B* **63**, 035109 (2001).

¹⁹It would also be useful to investigate the strength of the correlations in the charge channel using the same technique.

²⁰E. Y. Loh *et al.*, *Phys. Rev. B* **41**, 9301 (1990).